

# A novel trajectory-tracking control law for wheeled mobile robots

Sašo Blažič\*

University of Ljubljana, Faculty of Electrical Engineering, Tržaška 25, Ljubljana, Slovenia

## ARTICLE INFO

### Article history:

Received 7 April 2011

Received in revised form

7 June 2011

Accepted 17 June 2011

Available online 25 June 2011

### Keywords:

Mobile robot

Kinematic model

Lyapunov stability

Error model

## ABSTRACT

In this paper a novel kinematic model is proposed where the transformation between the robot posture and the system state is bijective. A nonlinear control law is constructed in the Lyapunov stability analysis framework. This control law achieves a global asymptotic stability of the system based on the usual requirements for reference velocities. The control law is extensively analysed and compared to some existing, globally stable control laws.

© 2011 Elsevier B.V. All rights reserved.

## 1. Introduction

The problem of the control of nonholonomic systems has attracted numerous investigations in the past. A thoroughly studied case, with great practical significance, is the wheeled mobile robot with a kinematic model similar to a unicycle [1]. The differentially driven mobile robots that are very common in practical applications also have the same kinematic model. Although many researchers coped with the more difficult problem of stabilising dynamic models for different types of mobile robots [2,3], the basic limitations of mobile robot control still come from their kinematic model, as shown in [4–6]. Kinematic control laws are also very important from the practical point of view, since the wheel-velocity control is often implemented locally on simple, micro-controller-based hardware, while the velocity command comes from high-level hardware that also provides the current control objective.

Traditionally, the problem of mobile robot control has been approached by point stabilisation [7] or by redefining the problem as a tracking control one [8]. There are also some approaches that tackle both problems simultaneously [9]. We believe that the tracking control approach is somewhat more appropriate, since the nonholonomic constraints and other control goals (obstacle avoidance, minimum travel time, minimum fuel consumption) are implicitly included in the path-planning procedure [10–12]. It is also easier to extend this approach to more complex schemes such as the control of mobile robot platoons [13]. Many control algorithms were proposed in the path-tracking framework, such

as PID [14], Lyapunov-based nonlinear controllers [15], adaptive controllers [2], model-based predictive controllers [16], fuzzy controllers [17–19], fuzzy neural networks [20], etc. Very often the fuzzy controllers take care of the high-level control [21] while in some cases they are implemented on chips or other industrial hardware [22,23]. Some approaches only guarantee local stability, while others also ensure global stability and global convergence under certain assumptions.

It is very important to find a (kinematic) control law that produces a smooth control signal. If this is not the case, the implementation on the dynamic model becomes impossible. Unfortunately, due to a discontinuity in the orientation error of  $\pm 180^\circ$ , quite often there is also a discontinuity in the angular-velocity command. This comes from the fact that the classical kinematic model is continuous with respect to orientation (there are no jumps at  $\pm\pi$ ), while in implementation the orientation is often mapped to the  $(-\pi, \pi]$  interval. In this paper a novel kinematic model is proposed that overcomes this difficulty, although it is of a higher order. A control law that achieves global asymptotic convergence to a predesigned path under some mild conditions is also proposed and compared to existing control laws.

The problem statement is given in Section 2. The new kinematic model and the corresponding error model are developed in Section 3. The Lyapunov control design is described in Section 4. In Section 5, several control algorithms are compared. The conclusions are stated in Section 6.

## 2. Problem statement

Assume a two-wheeled, differentially driven, mobile robot like the one depicted in Fig. 1, where  $(x, y)$  is the wheel-axis-centre position and  $\theta$  is the robot orientation. The kinematic motion

\* Tel.: +386 1 4768763; fax: +386 1 4264631.

E-mail address: [saso.blazic@fe.uni-lj.si](mailto:saso.blazic@fe.uni-lj.si).

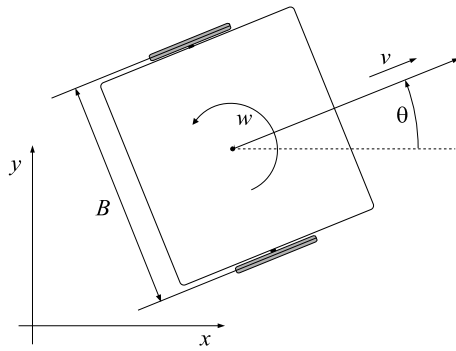


Fig. 1. Two-wheeled, differentially driven, mobile robot.

equations of such a mobile robot are equivalent to those of a unicycle. Robots with such an architecture have a nonholonomic constraint of the form:

$$\begin{bmatrix} -\sin\theta(t) & \cos\theta(t) \end{bmatrix} \begin{bmatrix} \dot{x}(t) \\ \dot{y}(t) \end{bmatrix} = 0 \quad (1)$$

resulting from the assumption that the robot cannot move in the lateral direction. Only the first-order kinematic model of the system will be treated in this paper:

$$\dot{q} = \begin{bmatrix} \dot{x} \\ \dot{y} \\ \dot{\theta} \end{bmatrix} = \begin{bmatrix} \cos\theta & 0 \\ \sin\theta & 0 \\ 0 & 1 \end{bmatrix} \begin{bmatrix} v \\ w \end{bmatrix} \quad (2)$$

where  $q^T(t) = [x(t) \ y(t) \ \theta(t)]$  is the vector of generalised coordinates, while  $v$  and  $w$  are the translational and the angular velocities, respectively, of the system in Fig. 1. The velocities of the right and the left wheels of the robot are  $v_R = v + \frac{wB}{2}$  and  $v_L = v - \frac{wB}{2}$ , respectively, where  $B$  is the robot inter-wheel distance. The control design goal is to follow the virtual robot or the reference trajectory, defined by

$$q_r^T(t) = [x_r(t) \ y_r(t) \ \theta_r(t)] \quad (3)$$

where  $q_r(t)$  is a priori known and smooth. It is very easy to show that the system (2) is flat [24], with the flat outputs being  $x$  and  $y$ . Consequently, (3) can be produced by the uniformly continuous control inputs  $v_r(t)$  and  $w_r(t)$  in the absence of initial conditions, parasitic dynamics and external disturbances. The goal is to design a feedback controller to achieve the tracking and the tracking should be asymptotic under the persistency of excitation (PE) through  $v_r(t)$  or  $w_r(t)$ .

### 3. Error model of the mobile robot kinematics

The posture error is not given in the global coordinate system, but rather as an error in the local coordinate system of the robot:  $e_x$  gives the error in the direction of driving,  $e_y$  gives the error in the lateral direction, and  $e_\theta$  gives the error in the orientation. The posture error  $e = [e_x \ e_y \ e_\theta]^T$  is determined using the actual posture  $q = [x \ y \ \theta]^T$  and the reference posture  $q_r = [x_r \ y_r \ \theta_r]^T$ :

$$\begin{bmatrix} e_x \\ e_y \\ e_\theta \end{bmatrix} = \begin{bmatrix} \cos\theta & \sin\theta & 0 \\ -\sin\theta & \cos\theta & 0 \\ 0 & 0 & 1 \end{bmatrix} (q_r - q). \quad (4)$$

#### 3.1. Third-order error model of the system

From (2) and (4) and assuming that the virtual robot has a kinematic model similar to (2), the posture-error model can be written as follows:

$$\begin{bmatrix} \dot{e}_x \\ \dot{e}_y \\ \dot{e}_\theta \end{bmatrix} = \begin{bmatrix} \cos e_\theta & 0 \\ \sin e_\theta & 0 \\ 0 & 1 \end{bmatrix} \begin{bmatrix} v_r \\ w_r \end{bmatrix} + \begin{bmatrix} -1 & e_y \\ 0 & -e_x \\ 0 & -1 \end{bmatrix} u. \quad (5)$$

The transformation (4) is theoretically imposed by the group operation, noting that the model (2) is a system in the Lie group  $SE(2)$  [5]. The approach itself was adopted in [8], where the authors also proposed PID control for the stabilisation of the robot at the reference posture. Later, many authors used the error model (5) for the tracking control design.

Very often, e.g., [14], the following control  $u$  is used to solve the tracking problem:

$$u = \begin{bmatrix} v \\ w \end{bmatrix} = \begin{bmatrix} v_r \cos e_\theta + v_b \\ w_r + w_b \end{bmatrix} \quad (6)$$

where  $u_b^T = [v_b \ w_b]$  is the feedback signal to be determined later. Inserting the control (6) into (5), the resulting model is given by:

$$\begin{aligned} \dot{e}_x &= w_r e_y - v_b + e_y w_b \\ \dot{e}_y &= -w_r e_x + v_r \sin e_\theta - e_x w_b \\ \dot{e}_\theta &= -w_b. \end{aligned} \quad (7)$$

#### 3.2. Fourth-order error model of the system

The problem of using the third-order error model presented in the previous section is that the transformation between the robot posture and the error model is not bijective. This can be observed from the fact that any error state  $[e_x \ e_y \ e_\theta + 2k\pi]^T$  for fixed  $e_x, e_y, e_\theta$ , and for arbitrary  $k \in \mathbb{Z}$  corresponds to the same robot posture. To say this more clearly: If we take any robot posture and rotate the robot for any multiple of  $360^\circ$ , the same robot posture is obtained (the sensors would not observe any difference between the two postures). Consequently, by just observing the robot posture it is impossible to deduce the orientation error. In practical control implementations the orientation error is often mapped onto the interval  $(-\pi, \pi]$  to somehow overcome the above mentioned bijectivity problem. The side effect of this is that the (angular-velocity) control signal often expresses discontinuity when the orientation error of  $\pm\pi$  is crossed (this will be shown in the examples at the end of the paper). Discontinuous velocity control signals are even more problematic because of the implementation on the real dynamic system.

The bijectivity between the robot posture and the states of the system should be therefore reflected in the kinematic model of the system and also in the error model of the system. This can be achieved by increasing the order of the system to 4. The variable  $\theta(t)$  from the original kinematic model (2) is exchanged by two new variables  $s(t) = \sin(\theta(t))$  and  $c(t) = \cos(\theta(t))$ . Their derivatives are:

$$\begin{aligned} \dot{s}(t) &= \cos(\theta(t))\dot{\theta}(t) = c(t)w(t) \\ \dot{c}(t) &= -\sin(\theta(t))\dot{\theta}(t) = -s(t)w(t). \end{aligned} \quad (8)$$

The new kinematic model is then obtained:

$$\dot{q} = \begin{bmatrix} \dot{x} \\ \dot{y} \\ \dot{s} \\ \dot{c} \end{bmatrix} = \begin{bmatrix} c & 0 \\ s & 0 \\ 0 & c \\ 0 & -s \end{bmatrix} \begin{bmatrix} v \\ w \end{bmatrix}. \quad (9)$$

The new error states are defined as

$$\begin{aligned} e_x &= c(x_r - x) + s(y_r - y) \\ e_y &= -s(x_r - x) + c(y_r - y) \\ e_s &= \sin(\theta_r - \theta) = s_r c - c_r s \\ e_{\cos} &= \cos(\theta_r - \theta) = c_r c + s_r s. \end{aligned} \quad (10)$$

After the differentiation of Eq. (10) and some manipulations, the following system is obtained.

$$\begin{aligned}\dot{e}_x &= v_r e_{\cos} - v + e_y w \\ \dot{e}_y &= v_r e_s - e_x w \\ \dot{e}_s &= w_r e_{\cos} - e_{\cos} w \\ \dot{e}_{\cos} &= -w_r e_s + e_s w.\end{aligned}\quad (11)$$

Like in (6),  $v = v_r e_{\cos} + v_b$  and  $w = w_r + w_b$  will be used in the control law. The control goal is to drive  $e_x$ ,  $e_y$ , and  $e_s$  to 0. The variable  $e_{\cos}$  is obtained as the cosine of the error in the orientation and should be driven to 1. This is why a new error will be defined as  $e_c = e_{\cos} - 1$  and the final error model of the system is now:

$$\begin{aligned}\dot{e}_x &= w_r e_y - v_b + e_y w_b \\ \dot{e}_y &= -w_r e_x + v_r e_s - e_x w_b \\ \dot{e}_s &= -e_c w_b - w_b \\ \dot{e}_c &= e_s w_b.\end{aligned}\quad (12)$$

#### 4. Lyapunov-based control design

A controller that achieves asymptotic stability of the error model (12) will be developed based on a Lyapunov approach. A very straightforward idea would be to use a Lyapunov function of the type

$$V_0 = \frac{k}{2} (e_x^2 + e_y^2) + \frac{1}{2} (e_s^2 + e_c^2) \quad (13)$$

however, a slightly more complex function will be proposed here, which also includes the function (13) as a special case. The following Lyapunov-function candidate is proposed to achieve the control goal:

$$V = \frac{k}{2} (e_x^2 + e_y^2) + \frac{1}{2(1 + \frac{e_c}{a})} (e_s^2 + e_c^2) \quad (14)$$

where  $k > 0$  and  $a > 2$  are constants. Note that the range of the function  $e_c = \cos(\theta_r - \theta) - 1$  is  $[-2, 0]$ , and therefore

$$\begin{aligned}0 < \frac{a-2}{a} \leq 1 + \frac{e_c}{a} \leq 1 \\ 1 \leq \frac{1}{1 + \frac{e_c}{a}} \leq \frac{a}{a-2}.\end{aligned}\quad (15)$$

Due to (15) the function  $V$  in (14) is lower-bounded by the function  $V_0$  in (13). Since the latter is of class  $\mathcal{X}$ ,  $V$  fulfils the conditions for the Lyapunov function. The role of  $(1 + \frac{e_c}{a})$  will be explained later on. The function  $V$  can be simplified by using the following:

$$e_s^2 + e_c^2 = e_s^2 + (e_{\cos} - 1)^2 = 2 - 2e_{\cos} = -2e_c. \quad (16)$$

Taking into account the equations of the error model (12) and (16), the derivative of  $V$  in (14) is:

$$\begin{aligned}\dot{V} &= -k e_x v_b + k v_r e_y e_s + \frac{1}{2(1 + \frac{e_c}{a})} (-2e_s w_b) + \frac{-\frac{1}{a} e_s w_b (-2e_c)}{2(1 + \frac{e_c}{a})^2} \\ &= -k e_x v_b + e_s \left( k v_r e_y - \frac{w_b}{(1 + \frac{e_c}{a})} \right).\end{aligned}\quad (17)$$

In order to make  $\dot{V}$  negative semi-definite, the following control law is proposed:

$$\begin{aligned}v_b &= k_x e_x \\ w_b &= k v_r e_y \left(1 + \frac{e_c}{a}\right)^2 + k_s e_s \left[\left(1 + \frac{e_c}{a}\right)^2\right]^n\end{aligned}\quad (18)$$

where  $k_x(t)$  and  $k_s(t)$  are positive functions, while  $n \in \mathbb{Z}$ . For practical reasons  $n$  is a small number (usually  $-2, -1, 0, 1$  or  $2$

are good choices). By taking into account the control law (18), the function  $\dot{V}$  becomes:

$$\dot{V} = -k k_x e_x^2 - k_s e_s^2 \left[\left(1 + \frac{e_c}{a}\right)^2\right]^{n-1}. \quad (19)$$

Two very well-known lemmas will be used in the proof of a theorem in this section. The first one is Barbālat's lemma and the other one is a derivation of Barbālat's lemma. Both lemmas are taken from [25] and are given below for the sake of completeness.

**Lemma 1 (Barbālat's Lemma).** *If  $\lim_{t \rightarrow \infty} \int_0^t f(\tau) d\tau$  exists and is finite, and  $f(t)$  is a uniformly continuous function, then  $\lim_{t \rightarrow \infty} f(t) = 0$ .*

**Lemma 2.** *If  $f, \dot{f} \in \mathcal{L}_\infty$  and  $f \in \mathcal{L}_p$  for some  $p \in [1, \infty)$ , then  $f(t) \rightarrow 0$  as  $t \rightarrow \infty$ .*

In Lemma 2 the  $\mathcal{L}_p$  norm of a function  $f(t)$  is used. It is defined as:

$$\|f\|_p = \left( \int_0^\infty |f(\tau)|^p d\tau \right)^{1/p} \quad (20)$$

where  $|\cdot|$  denotes the vector (scalar) length. If the above integral exists (is finite), the function  $f(t)$  is said to belong to  $\mathcal{L}_p$ . Limiting  $p$  towards infinity provides a very important class of functions  $\mathcal{L}_\infty$ —bounded functions.

**Theorem 1.** *If the control law (18) is applied to the system (12) where  $k$  is a positive constant,  $a > 2$  is a constant,  $k_x$  and  $k_s$  are positive bounded functions, and the reference velocities  $v_r$  and  $w_r$  are bounded, then the tracking errors  $e_x$ ,  $e_s$ , and  $e_c$  converge to 0. The convergence of  $e_y$  to 0 is guaranteed, provided that at least one of the two conditions is met:*

1.  $v_r$  is uniformly continuous and does not go to 0 as  $t \rightarrow \infty$ , while  $k_s$  is uniformly continuous,
2.  $w_r$  is uniformly continuous and does not go to 0 as  $t \rightarrow \infty$ , while  $v_r$ ,  $k_x$ , and  $k_s$  are uniformly continuous.

**Proof.** It follows from (19) that  $\dot{V} \leq 0$ , and therefore the Lyapunov function is non-increasing. Consequently, the following can be concluded:

$$e_x, e_y, e_s, e_c \in \mathcal{L}_\infty. \quad (21)$$

Based on (21), it follows from (18) that the control signals are bounded, and from (12) that the derivatives of the errors are bounded:

$$v_b, w_b, \dot{e}_x, \dot{e}_y, \dot{e}_s, \dot{e}_c \in \mathcal{L}_\infty \quad (22)$$

where we also took into account that  $v_r, w_r, k, k_x, k_s$ , and  $(1 + \frac{e_c}{a})^{2n}$  are bounded. It follows from Eqs. (21) and (22) that  $e_x, e_y, e_s$ , and  $e_c$  are uniformly continuous (note that the easiest way to check the uniform continuity of  $f(t)$  on  $[0, \infty)$  is to see if  $f, \dot{f} \in \mathcal{L}_\infty$ ).

In order to show the asymptotic stability of the system, let us first calculate the following integral:

$$\begin{aligned}\int_0^\infty \dot{V} dt &= V(\infty) - V(0) \\ &= - \int_0^\infty k k_x e_x^2 dt - \int_0^\infty k_s e_s^2 \left[\left(1 + \frac{e_c}{a}\right)^2\right]^{n-1} dt\end{aligned}\quad (23)$$

where the notation  $V(t)$  is used although  $V$  does not depend on  $t$  explicitly. Since  $V$  is a positive definite function, the following inequality holds:

$$\begin{aligned}V(0) &\geq \int_0^\infty k k_x e_x^2 dt + \int_0^\infty k_s e_s^2 \left[\left(1 + \frac{e_c}{a}\right)^2\right]^{n-1} dt \\ &\geq k \underline{k}_x \int_0^\infty e_x^2 dt + k_s \underline{k}_s \int_0^\infty e_s^2 dt\end{aligned}\quad (24)$$

where the lower bounds of the functions  $k_x(t)$ ,  $k_s(t)$ , and  $\left(1 + \frac{e_c(t)}{a}\right)^{2(n-1)}$  are introduced

$$\begin{aligned} 0 < \underline{k}_x &\leq k_x(t) \quad t \in \mathbb{R} \\ 0 < \underline{k}_s &\leq k_s(t) \quad t \in \mathbb{R} \\ 0 < \underline{L} &\leq \left(1 + \frac{e_c(t)}{a}\right)^{2(n-1)} \quad t \in \mathbb{R} \end{aligned} \quad (25)$$

and two cases can be distinguished to determine the value of  $\underline{L}$  due to (15):

$$\underline{L} = \begin{cases} 1 & n \leq 1 \\ \left(\frac{a-2}{a}\right)^{2(n-1)} & n > 1. \end{cases} \quad (26)$$

It follows from (24) that  $e_x, e_s \in \mathcal{L}_2$ . Applying Lemma 2, the convergence of  $e_x(t)$  and  $e_s(t)$  to 0 follows immediately. When  $e_s$  is 0,  $e_c$  can be either 0 or  $-2$  since  $e_s$  and  $(e_c + 1)$  are the sine and the cosine, respectively, of the same argument. Due to  $e_s \rightarrow 0$ , it follows from (12) that  $\dot{e}_c \rightarrow 0$  and consequently the limit  $\lim_{t \rightarrow \infty} e_c(t)$  exists and is either 0 or  $-2$ .

Until now we only established the convergence of  $e_x(t)$  and  $e_s(t)$  to 0, while  $e_c(t)$  was shown to converge either to 0 or to  $-2$ . To show the convergence of  $e_y(t)$  to 0, at least one of the conditions 1 or 2 of Theorem 1 have to be fulfilled. Let us first analyse the condition 1. Applying Lemma 1 to  $\dot{e}_s(t)$  ensures that  $\lim_{t \rightarrow \infty} \dot{e}_s(t) = 0$  if  $\lim_{t \rightarrow \infty} e_s(t)$  exists and is finite (which has already been proven) and  $\dot{e}_s(t)$  is uniformly continuous. The latter is true (see (12)) if  $(e_c + 1)w_b$  is uniformly continuous. It has already been shown that  $e_c$  is uniformly continuous. The feedback control for the angular velocity  $w_b$  defined in (18) is uniformly continuous since  $k_s$  and  $v_r$  are uniformly continuous from the assumption in condition 1 of the theorem. The statement  $\lim_{t \rightarrow \infty} \dot{e}_s(t) = 0$ , which is identical to

$$\lim_{t \rightarrow \infty} \left( - (e_c(t) + 1) w_b(t) \right) = 0 \quad (27)$$

has therefore been proven. Since  $(e_c(t) + 1)$  converges to 1 or to  $-1$ , the following can be concluded from (18):

$$\begin{aligned} \lim_{t \rightarrow \infty} w_b &= \lim_{t \rightarrow \infty} \left( k v_r e_y \left(1 + \frac{e_c}{a}\right)^2 + k_s e_s \left[ \left(1 + \frac{e_c}{a}\right)^2 \right]^n \right) \\ &= 0. \end{aligned} \quad (28)$$

The factor  $\left(1 + \frac{e_c}{a}\right)$  can converge either to 1 or to  $\left(1 - \frac{2}{a}\right)$ , but is always strictly positive and bounded. Since the same holds for  $k_s$ , while it was shown that  $e_s$  converges to 0, the whole second term of  $w_b$  in Eq. (28) also converges to 0. In the first term  $k$  is a finite constant,  $\left(1 + \frac{e_c}{a}\right)^2$  is bounded and strictly positive, while  $v_r$  is also bounded and does not diminish as  $t \rightarrow \infty$  due to the assumption in the condition 1. Consequently, the convergence of  $e_y$  to 0 follows.

For the second case (condition 2) Barbălat's lemma (Lemma 1) is applied to  $\dot{e}_x$  in Eq. (12) after inserting the control law for  $v_b$  (18):

$$\dot{e}_x = w_r e_y - k_x e_x + e_y w_b. \quad (29)$$

In order to show that  $\lim_{t \rightarrow \infty} \dot{e}_x = 0$  we again have to guarantee that all the signals on the right-hand side of Eq. (29) are uniformly continuous. We have seen that  $e_x$  and  $e_y$  are uniformly continuous,  $w_r$  and  $k_x$  are uniformly continuous from the assumption of the condition 2, while  $w_b$  is uniformly continuous if  $k_s$  and  $v_r$  are uniformly continuous. The latter two conditions also guarantee that  $\lim_{t \rightarrow \infty} w_b = 0$  as shown before. Since  $e_x$  and  $w_b$  converge to 0 while  $k_x$  and  $e_y$  are bounded, the last two terms in Eq. (29) go to 0 as  $t$  goes to infinity. Consequently, the product  $w_r e_y$  also goes to 0. Since  $w_r$  does not go to 0,  $e_y$  has to go to 0.

It is somehow more difficult to prove the convergence of  $e_c$  to 0. However, it has already been shown that  $e_c$  converges either to 0 or to  $-2$ , and it is easy to show that  $e_c$  will converge to 0 if the initial condition of the error vector is in the vicinity of the origin or the design parameter  $a$  is sufficiently close to 2. The error  $e_c$  converges to 0 asymptotically if one of the following conditions is satisfied:

- $V(0) \leq 2$ , or
- $V(0) > 2$  and  $a < \frac{2V(0)}{V(0)-2}$ .

To prove this statement, let us calculate the value of the Lyapunov function  $V$  in  $e_{-2} = [0 \ 0 \ 0 \ -2]^T$ :

$$V_{-2} = V|_{e=e_{-2}} = \frac{1}{2 \left(1 + \frac{e_c}{a}\right)} e_c^2 \Big|_{e_c=-2} = \frac{2a}{a-2} > 2. \quad (30)$$

It is easy to show that  $V(0) < V_{-2}$  if one of the above two conditions is satisfied. Among all the points that share the same  $e_c = -2$ ,  $e_{-2}$  is the point with the lowest  $V$ . Since  $V$  is a monotonically non-increasing function, the system can never reach any point with  $e_c = -2$ . Thus, it is only possible that  $e_c$  converges to 0.

Now let us assume that  $e_c$  is in the vicinity of  $-2$ . Upon inserting  $w_b$  from Eq. (18),  $\dot{e}_c$  in Eq. (12) becomes:

$$\dot{e}_c = e_s w_b = k v_r e_y e_s \left(1 + \frac{e_c}{a}\right)^2 + k_s e_s^2 \left(1 + \frac{e_c}{a}\right)^{2n}. \quad (31)$$

The second term in Eq. (31) is always positive. The error  $e_c$  will increase and thus be repelled from  $e_c = -2$  if the product  $v_r e_y e_s$  is positive. If this is not satisfied, then  $e_c$  will still increase if  $|v_r e_y|$  is small enough (the second term is dominant in Eq. (31)):

$$|v_r e_y| < \frac{k_s}{k} |e_s| \left(1 + \frac{e_c}{a}\right)^{2(n-1)} \Rightarrow \dot{e}_c > 0. \quad (32)$$

Even if this is not the case, the analysis in the vicinity of  $e_c = -2$  will show that this equilibrium point is repelling. The errors  $e_x$  and  $e_s$  always converge to 0 and we can say that after some time they belong to  $O(\varepsilon)$  where  $\varepsilon$  is sufficiently small. It is easy to conclude from (12) that the derivatives of the errors then become:

$$\begin{aligned} \dot{e}_y &= O(\varepsilon) \\ \dot{e}_s &= (-e_c - 1) k v_r e_y \left(1 + \frac{e_c}{a}\right)^2 + O(\varepsilon). \end{aligned} \quad (33)$$

Now we are interested in the derivative of  $v_r e_y e_s$ :

$$\begin{aligned} \frac{d}{dt} (v_r e_y e_s) &= \dot{v}_r e_y e_s + v_r \dot{e}_y e_s + v_r e_y \dot{e}_s \\ &= O(\varepsilon) + O(\varepsilon^2) + (-e_c - 1) k v_r^2 e_y^2 \left(1 + \frac{e_c}{a}\right)^2 + O(\varepsilon). \end{aligned} \quad (34)$$

We can see that in the vicinity of  $e_c = -2$  the dominant term in Eq. (34) is always positive and  $\dot{e}_c$  in (31) also eventually becomes positive. Even if for a short time the error  $e_c$  is approaching  $-2$ , it is always repelled after that. Note that this happens when  $e_s$  and  $v_r e_y$  are of the opposite sign (if they are of the same sign  $e_c$  always increases). From (12) it can be concluded that  $e_s$  will then move in the direction of changing its sign. But it has to cross  $e_s = 0$  when  $e_c$  becomes  $-2$ . This is why the error  $e_c$  actually crosses  $e_c = -2$  but it is immediately repelled from it. The solution  $e_c = -2$  is therefore an unstable equilibrium point.

Since  $e_c$  cannot be attracted to  $-2$  for a longer time, it has to eventually be driven to 0 because this is the only alternative.  $\square$

## 5. Comparison of different control laws

The proposed method has been extensively tested and compared to the existing methods from the literature. The first one

is from [14] and the other one is inspired by Samson's work [15]. These algorithms were chosen because they were both designed using Lyapunov stability theory. The Lyapunov functions used therein have the same limit around the zero error in orientation ( $e_\theta = 0$ ). The control law proposed in [14] is:

$$\begin{aligned} v_b &= k_x e_x \\ w_b &= k v_r e_y + k_s \sin e_\theta. \end{aligned} \quad (35)$$

Actually, there was also a third factor  $v_r$  in the second term of  $w_b$  which is not normally used in the recent papers that cite this approach since additional assumptions about  $v_r$  are needed. On the other hand,  $v_r$  can also be included in  $k_s$  if the requirements are met. Note that the control law (35) can be easily developed if the most straightforward Lyapunov function  $V_0$  from (13) is used in the controller design procedure. Note also that the control law (35) is a special case of (18) when  $a$  limits to infinity.

The control law due to Samson is:

$$\begin{aligned} v_b &= k_x e_x \\ w_b &= k v_r e_y \frac{\sin e_\theta}{e_\theta} + k_s e_\theta. \end{aligned} \quad (36)$$

In our simulation experiments the orientation error  $e_\theta$  in (36) was always mapped to the interval  $(-\pi, \pi]$  to make the comparison fair. It is easy to see that all three control laws given in Eqs. (18), (35) and (36) that will be compared in the paper have the same limit around  $e_\theta = 0$  and it is therefore fair to use the same control gains—in our case we shall use  $k = 10$ ,  $k_x = 10$ , and  $k_s = 10$ .

The form of the control laws suggests that the role of  $v_b$  is always the reduction of  $e_x$ , while  $w_b$  needs to cater for the remaining two errors. A very simplified explanation is that the first term in  $w_b$  takes care of the lateral error, while the second term is responsible for the orientation error. In reality, the problems are much more complicated, due to the nonholonomic nature of the system. Nevertheless, we can still be sure of certain facts:

- The feedback  $v_b$  is the same in all three control laws that have been compared, and therefore we cannot expect any drastic differences in performance.
- The control laws (18) and (35) are continuous with respect to the orientation error (at the orientation error of  $\pm\pi$ ) while the control law (36) does not share this property. This is a problem of the latter approach since the implementation of the discontinuous control law on a dynamic model becomes questionable.
- Let us denote the “gain” from  $e_y$  to  $w_b$  by  $g_y(t) \triangleq |w_b(t)|/|e_y(t)|_{e_\theta(t)=0}$ . Additionally, the superscripts  $p$ ,  $k$ , and  $s$  denote the proposed control law (18), Kanayama's control law (35), and Samson's control law (36), respectively. Among the three control laws compared,  $g_y^k$  is always the highest. It is easy to show that if  $a \geq 6$ ,  $g_y^p$  is always larger than  $g_y^s$ . If  $2 < a < 6$ ,  $g_y^s > g_y^p$  when  $e_\theta$  is small, and  $g_y^s < g_y^p$  when  $e_\theta$  is large.
- Let us denote the “gain” from  $e_\theta$  to  $w_b$  by  $g_\theta(t) \triangleq |w_b(t)|/|e_\theta(t)|_{e_y(t)=0}$ . The superscripts are the same as above. If  $n > 0$ ,  $g_\theta^p < g_\theta^k < g_\theta^s$ . If  $n = 0$ ,  $g_\theta^p = g_\theta^k < g_\theta^s$ . If  $n$  is negative, then  $g_\theta^k$  is the lowest. The comparison between Samson's control law and the proposed one depends on the choice of design parameters. If  $a \leq 6|n|$ ,  $g_\theta^p < g_\theta^s$ . If  $a > 6|n|$ , the comparison also depends on the orientation error:  $g_\theta^p > g_\theta^s$  for small  $e_\theta$  and  $g_\theta^p < g_\theta^s$  for large  $e_\theta$ .

If we try to summarise the above analysis we can see that for  $n > 0$ , the proposed control law always has the lowest gain  $g_\theta$ , while either Samson's law or the proposed one have the lowest  $g_y$  gain. This means that we can expect lower control effort from these two laws, while Kanayama's law will exert more control action.

An extensive simulation study was performed to compare all the approaches under the same circumstances. The reference

**Table 1**  
Cost functions of individual control laws.

$i$	$\bar{C}_e^i$	$\bar{C}_v^i$	$\bar{C}_w^i$	$N_\pi^i$
1	1.4894	1.0186	1.8870	98
2	1.3693	1.0046	1.7706	98
3	1.0742	1.0628	1.7594	483
4	1.4426	1.0133	1.8355	98
5	1.3336	1.0066	1.6903	154
6	1.0599	1.0667	1.7651	500
7	1.4126	1.0184	1.5696	98
8	1.2591	1.0217	1.5912	265
9	1.0471	1.0696	1.7655	508
10	4.5709	1.2081	1	98
11	1.0881	1.0773	1.5766	499
12	1.0345	1.0725	1.7658	516
13	7.3737	1.5574	1.1021	98
14	1	1.1319	1.5885	758
15	1.0226	1.0754	1.7669	524
16	1.3591	1	1.7534	0
17	1.0328	1.0724	1.7763	517

trajectory is the same in all the simulation runs:

$$\begin{aligned} x_r(t) &= \cos(\omega_0 t) \\ y_r(t) &= \sin(2\omega_0 t) \end{aligned} \quad (37)$$

with  $\omega_0 = 0.34$ . The simulation run always started at  $t = 0$  and finished at  $t = \frac{2\pi}{\omega_0}$ . The control signals  $v_b$  and  $w_b$  were saturated to  $\pm 10$ . The simulation experiment was conducted with different initial conditions. The possible initial conditions of the mobile robot were

$$\begin{aligned} e_x(0), e_y(0) &\in I_{xy} = \{-2, -1.5, -1, -0.7, -0.5, \\ &\quad -0.3, -0.1, 0.1, 0.3, 0.5, 0.7, 1, 1.5, 2\} \\ e_\theta(0) &\in I_\theta = \left\{ \frac{l\pi}{12} \mid l = -11, -10, \dots, 12 \right\}. \end{aligned} \quad (38)$$

For each simulation run the following cost function was calculated:

$$i C_e^{xy\theta} = \int_0^{\frac{2\pi}{\omega_0}} \left[ \frac{k}{2} e_x^2(t) + \frac{k}{2} e_y^2(t) + \frac{1}{2} e_\theta^2(t) \right] dt \quad (39)$$

where  $x$ ,  $y$ , and  $\theta$  denote the respective initial conditions, while  $i$  denotes the index of the control law. Seventeen different control laws were tested: Eq. (35) corresponds to  $i = 17$ , Eq. (36) corresponds to  $i = 16$ , and Eq. (18) corresponds to  $i = 1, \dots, 15$ , where 15 variations with  $n \in \{-2, -1, 0, 1, 2\}$  and  $a \in \{2.1, 7100\}$  were used:  $n = -2$ ,  $a = 2.1$  correspond to  $i = 1$ ,  $n = -2$ ,  $a = 7$  correspond to  $i = 2$ , and so on. For each variation of the initial conditions in (38), seventeen simulation experiments were conducted with seventeen different control laws, meaning that the total number of simulation runs was  $14 \times 14 \times 24 \times 17$ .

Note that the integral of the Lyapunov function used for the development of (36) was used (for small errors in the orientation all three Lyapunov functions have the same limit) for the cost function of an individual simulation run (39). The overall cost function of a certain control law  $i$  was simply the sum of all the individual cost functions:

$$C_e^i = \sum_{x \in I_{xy}} \sum_{y \in I_{xy}} \sum_{\theta \in I_\theta} (i C_e^{xy\theta}). \quad (40)$$

Whenever the performance of a control law is discussed, it is necessary to check for the control effort. Analogously with Eqs. (39) and (40),  $C_v^i$  and  $C_w^i$  are defined as the sums of the integrals of  $v_b^2$  and  $w_b^2$ , respectively. Table 1 shows the cost functions  $\bar{C}_e^i$ ,  $\bar{C}_v^i$ , and  $\bar{C}_w^i$  (these are obtained by normalising the respective cost functions with the best one in the column) for all 17 control laws. The smallest total error  $C_e^i$  (or  $\bar{C}_e^i$ ) is achieved by the proposed control law with  $n = 2$  and  $a = 7$  ( $i = 14$ ), followed closely

**Table 2**  
The columns show the ranking (according to  ${}^l C_e^i$ ) of the control laws for all the simulation runs with  $e_\theta(0) = l\pi/12$  (the first row shows the index  $i$  of the best control law).

$l =$											
–12	–11	–10	–9	–8	–7	–6	–5	–4	–3	–2	–1
1	1	6	17	15	14	14	14	14	14	14	14
4	4	17	9	17	15	11	15	15	15	13	13
2	17	9	12	12	11	15	10	17	17	15	15
16	2	3	6	9	12	12	11	12	12	17	17
3	6	12	15	6	17	17	12	11	9	12	12
5	3	15	3	11	9	9	17	9	11	9	9
17	9	1	11	3	6	6	9	10	6	11	11
6	5	4	1	14	3	3	6	6	3	6	6
9	12	8	4	1	7	10	3	3	13	3	3
12	15	7	8	4	8	8	8	8	10	10	10
15	16	2	7	7	16	7	7	5	8	8	8
8	7	16	2	2	5	5	5	13	5	5	5
11	8	5	16	16	2	16	16	16	16	16	16
14	11	11	5	5	4	2	2	7	2	2	2
7	14	14	14	8	1	4	4	2	7	7	7
10	10	10	10	10	10	1	1	4	4	4	4
13	13	13	13	13	13	13	13	1	1	1	1

$l =$											
0	1	2	3	4	5	6	7	8	9	10	11
14	14	14	14	14	14	14	14	15	17	6	1
13	13	15	15	15	10	11	11	17	9	3	4
15	15	17	17	12	15	15	15	12	12	17	2
17	17	12	12	17	11	12	12	9	6	9	16
12	12	9	9	10	12	17	17	6	15	12	5
9	9	6	11	11	17	9	9	3	3	1	17
11	11	11	6	9	9	6	6	11	11	15	3
6	6	3	3	6	6	10	3	1	1	4	6
3	3	10	10	3	3	3	7	7	4	7	9
10	10	13	8	8	8	8	8	4	7	2	12
8	8	8	5	5	7	7	5	2	8	8	15
5	5	5	13	7	5	5	16	16	2	5	7
16	16	16	16	16	16	16	2	5	16	16	8
2	2	2	2	2	2	2	4	8	5	11	11
7	7	7	7	4	4	4	1	14	14	14	14
4	4	4	4	13	1	1	10	10	10	10	10
1	1	1	1	1	13	13	13	13	13	13	13

by the combination  $n = 2$  and  $a = 100$  ( $i = 15$ ), Nakayama's law ( $i = 17$ ), and the combination  $n = 1$  and  $a = 100$  ( $i = 12$ ). We can also see that the control laws with  $a = 2.1$ ,  $n = 1$  ( $i = 10$ ) and especially with  $a = 2.1$ ,  $n = 2$  ( $i = 13$ ) showed really bad results. The problem lies in the fact that in these cases the control  $w_b$  is practically switched off when the orientation error is large. The convergence is therefore very slow. This is why the control effort  $\bar{C}_w^i$  is so low in these two cases. Due to the slow convergence in these two cases, these approaches are also the worst when only  $\bar{C}_v^i$  is observed. In other cases, no big differences among  $\bar{C}_v^i$  can be found, as expected. Perhaps we should note that the control law with the best total error ( $i = 14$ ) is slightly worse in this respect than the others. When comparing  $\bar{C}_w^i$  and leaving out  $i = 10$  and  $i = 13$ , which show very bad performance, the lowest overall control effort is connected with the proposed control laws with  $n = 0$ . If we were to choose the best control law, then we would probably select the one with  $i = 15$ , which shows very good overall performance. Kanayama's control law is very close while Samson's results are not so good (the only exception is the control effort for the linear velocity, but even here the differences are small). The last column in Table 1 shows the total number of crossings of the  $\pm 180^\circ$  orientation error. It is interesting to note that good overall performance is highly correlated with a large number of these crossings. It is obviously often advantageous to try to minimise the orientation error even though, for a short period of time, the orientation error is rising. Samson's control law never did this and yet its performance is bad.

Table 1 shows the average cost functions, but it is obvious that all the control laws behave quite differently when exposed to

different initial conditions (especially in orientation). To illustrate this, the cost function  $C_e^i$  was computed for each initial condition in orientation separately:

$${}^l C_e^i = \sum_{x \in I_{xy}, y \in I_{xy}, \theta = l\pi/12} ({}^i C_e^{xy\theta}). \quad (41)$$

To reduce the level of information, only the rankings with respect to  $l$  are shown in Table 2. One can notice immediately that for low orientation errors the high values of  $n$  are good, while for large initial orientation errors the negative values of  $n$  are better. The explanation is very simple. When  $n < 0$  the second term in  $w_b$  is the dominant one. This means that the main control goal is to reduce the error in the orientation, while the lateral error is not so important. Such a strategy is useful when the error in the orientation is high and it is necessary to reduce it quite quickly (otherwise the error in  $e_y$  can also increase due to the interconnection). When, on the other hand, the orientation error is low, it is more important to cope with  $e_y$ , which is a problematic error due to the nonholonomic constraints. We achieve the emphasis on the regulation of  $e_y$  when  $n > 0$ .

## 6. Conclusion

In this paper a novel kinematic model is proposed where the transformation between the robot posture and the system state is bijective. A novel control law is also proposed. It is designed within the Lyapunov stability framework. It is proven that the global asymptotic stability of the system is achieved under some

very mild conditions if the reference velocities satisfy the condition of persistent excitation.

An extensive simulation study was performed and the results of the proposed control law are compared to some control laws from the literature. The results of the simulation study also suggest that the parameters  $n$  and  $a$  of the proposed control law could be scheduled according to the orientation error. The possibility of adapting these parameters also exists since  $n$  could also be a real number, but this could lead to stability problems. These aspects are, therefore, a topic of future research.

## References

- [1] I. Kolmanovsky, N.H. McClamroch, Developments in nonholonomic control problems, *IEEE Control Systems Magazine* 15 (6) (1995) 20–36.
- [2] Z.-P. Jiang, H. Nijmeijer, Tracking control of mobile robots: a case study in backstepping, *Automatica* 33 (7) (1997) 1393–1399.
- [3] F. Pourboghrat, M.P. Karlsson, Adaptive control of dynamic mobile robots with nonholonomic constraints, *Computers & Electrical Engineering* 28 (4) (2002) 241–253.
- [4] R.W. Brockett, Asymptotic stability and feedback stabilization, in: *Differential Geometric Control Theory*, Birkhäuser, Boston, MA, 1983, pp. 181–191.
- [5] P. Morin, C. Samson, Control of nonholonomic mobile robots based on the transverse function approach, *IEEE Transactions on Robotics* 25 (5) (2009) 1058–1073.
- [6] D. Lizarraga, Obstructions to the existence of universal stabilizers for smooth control systems, *Mathematics of Control, Signals, and Systems, MCSS* 16 (2004) 255–277.
- [7] F. Pourboghrat, Exponential stabilization of nonholonomic mobile robots, *Computers & Electrical Engineering* 28 (5) (2002) 349–359.
- [8] Y. Kanayama, A. Nilipour, C. Lelm, A locomotion control method for autonomous vehicles, in: *Proceedings of the 1988 IEEE International Conference on Robotics and Automation*, Washington, DC, USA, vol. 2, 1988, pp. 1315–1317.
- [9] D. Bucciari, D. Perritaz, P. Mullhaupt, Z.-P. Jiang, D. Bonvin, Velocity-scheduling control for a unicycle mobile robot: theory and experiments, *IEEE Transactions on Robotics* 25 (2) (2009) 451–458.
- [10] S.M. LaValle, *Planning Algorithms*, Cambridge University Press, Cambridge, UK, 2006.
- [11] M. Lepetić, G. Klančar, I. Škrjanc, D. Matko, B. Potočnik, Time optimal path planning considering acceleration limits, *Robotics and Autonomous Systems* 45 (3–4) (2003) 199–210.
- [12] C. Pozna, F. Troester, R.-E. Precup, J.K. Tar, S. Preitl, On the design of an obstacle avoiding trajectory: method and simulation, *Mathematics and Computers in Simulation* 79 (7) (2009) 2211–2226.
- [13] G. Klančar, D. Matko, S. Blažič, A control strategy for platoons of differential drive wheeled mobile robot, *Robotics and Autonomous Systems* 59 (2) (2011) 57–64.
- [14] Y. Kanayama, Y. Kimura, F. Miyazaki, T. Noguchi, A stable tracking control method for an autonomous mobile robot, in: *Proceedings 1990 IEEE International Conference on Robotics and Automation*, Los Alamitos, CA, USA, vol. 1, 1990, pp. 384–389.
- [15] C. Samson, Time-varying feedback stabilization of car like wheeled mobile robot, *International Journal of Robotics Research* 12 (1) (1993) 55–64.
- [16] G. Klančar, I. Škrjanc, Tracking-error model-based predictive control for mobile robots in real time, *Robotics and Autonomous Systems* 55 (6) (2007) 460–469.
- [17] E.-H. Guechi, J. Lauber, M. Dambrine, G. Klančar, S. Blažič control design for non-holonomic wheeled mobile robots with delayed outputs, *Journal of Intelligent & Robotic Systems* 60 (3) (2010) 395–414.
- [18] T.H.S. Li, S.J. Chang, Autonomous fuzzy parking control of a car-like mobile robot, *IEEE Transactions on Systems, Man, and Cybernetics—Part A: Systems and Humans* 33 (4) (2003) 451–465.
- [19] Z.-G. Hou, A.-M. Zou, L. Cheng, M. Tan, Adaptive control of an electrically driven nonholonomic mobile robot via backstepping and fuzzy approach, *IEEE Transactions on Control Systems Technology* 17 (4) (2009) 803–815.
- [20] R.-J. Wai, C.-M. Liu, Design of dynamic petri recurrent fuzzy neural network and its application to path-tracking control of nonholonomic mobile robot, *IEEE Transactions on Industrial Electronics* 56 (7) (2009) 2667–2683.
- [21] E. Maalouf, M. Saad, H. Saliyah, A higher level path tracking controller for a four-wheel differentially steered mobile robot, *Robotics and Autonomous Systems* 54 (1) (2006) 23–33.
- [22] S.G. Tzafestas, K.M. Deliparaschos, G.P. Moustris, Fuzzy logic path tracking control for autonomous non-holonomic mobile robots: design of system on a chip, *Robotics and Autonomous Systems* 58 (8) (2010) 1017–1027.
- [23] R.-E. Precup, H. Hellendoorn, A survey on industrial applications of fuzzy control, *Computers in Industry* 62 (3) (2011) 213–226.
- [24] M. Fliess, J. Levine, P. Martin, P. Rouchon, Flatness and defect of nonlinear systems—introductory theory and examples, *International Journal of Control* 61 (6) (1995) 1327–1361.
- [25] P.A. Ioannou, J. Sun, *Robust Adaptive Control*, Prentice-Hall, 1996.



**Sašo Blažič** received the B.Sc., M. Sc., and Ph. D. degrees in 1996, 1999, and 2002, respectively, from the Faculty of Electrical Engineering, University of Ljubljana. His research interests include adaptive, fuzzy and predictive control of dynamical systems and modelling of nonlinear systems. He is also working in the area of mobile robotics with a stress on path planning and path following issues.